



MANUFACTURABILITY OF COMPOSITE PRESSURE VESSELS: APPLICATION OF NON-GEODESIC WINDING

Sotiris Koussios, Adriaan Beukers, Pyrrhos Stathis
Design & Production of Composite Structures
Faculty of Aerospace Engineering
Delft University of Technology

Keywords: *Filament winding, Pressure vessels, Non-Geodesics, Friction*

Abstract

The geodesic trajectories based design of optimal filamentary pressure vessels is a well-understood item. However, the roving geometry, as dictated by structural analysis in combination with exclusively application of geodesics, does not comply with the entire set of production process related requirements. The most important shortcoming is that the winding angle at the pole does not provide tangential fibre placement. This condition is essential for proceeding to the following wound circuits. In this paper we propose partial application of non-geodesic winding to overcome this problem. The outlined theory is based on the same set of parameters used for the analytical derivation of isotensoid meridian profiles.

1 Introduction

1.1 Background

Optimal filamentary composite pressure vessels provide significant advantages as compared to their steel-based counterparts [1, 2, 3]. They are able to realise significant weight reductions and improved impact performance, particularly in the case where the incorporated matrix is sufficiently flexible. The basic mechanism for composite pressure vessels relies on the alignment of the rovings with the principal stress direction on such a way that these rovings become equally loaded on tension only (isotensoid).

1.2 Problem Identification

Next to these advantages however, the design of such vessels is prone to particular limitations. The most important among them is the radius range in which the optimality is preserved. Namely, the entire meridian profile of an isotensoid is characterized by two parameters: the aspect ratio q and the dimensionless axial force r [2, 3, 4]. The q parameter is associated with the ratio of the maximum and minimum radius, and the parameter r with the external axial force as compared to the axial force that is generated by the internal pressure on the end cap (polar opening). Assuming geodesic winding, the requirement of reaching a winding angle of 90° at the polar areas is not always satisfied. With an exception for the parameter combination $r = -1/q$, the winding angle will never become equal to the abovementioned desired value [3]. This shortcoming is particularly important for small q values (polar opening radius close the equatorial one). The filament winding process however, requires perfectly tangent placement of the rovings when passing the polar areas of the vessel (winding angle = 90°). To overcome this contradiction, the designer has two options. The first one is to continue winding towards a smaller radius. However, this option requires adapted meridian profiles and bigger flanges. In this case, the optimality of the vessel is obviously not preserved and the weight increases. The second option is to apply non-geodesic winding on such a way that the desired winding angle is reached at exactly the minimal optimal radius. Although the optimality is once again not preserved, the construction of adapted flanges can be omitted and the expected reduction of structural performance can easily be quantified [5]. The derivation of such paths however, is not a simple task. Despite the overall presence of this problem when designing

composite pressure vessels, little attention has been drawn to a generic and flexible solution.

1.3 Proposed solution

In this paper we outline a stable and easily accessible solution procedure for the description of non geodesic trajectories, particularly applied on optimal filamentary composite pressure vessels. The roving paths are in this case parameterised in an elliptical coordinate system.

The reason for this choice is that the description of non-geodesic trajectories in the classical polar coordinates system is not an easy task [6]. The solution of the non-linear differential equation for non-geodesic trajectories is not stable and the singularity that rises when the winding angle approaches 90° does strongly influence the results. These problems are not strongly present when applying elliptical coordinate systems. At the same time, the implemented coordinate system forms a solid basis for an elegant description of the isotensoid profile itself [2, 3].

1.4 Outline

After a short outline of the theory for optimal filamentary vessels (section 2), the governing equations are presented in elliptical coordinates. Next to the optimal meridian profile, additional items like winding angles, parallel angle development and roving length are derived. The determination of these quantities is necessary for the elaboration of the winding process in practice [7, 8].

Next, (section 3) with standard tools from geometry, the differential equation for non-geodesic trajectories is presented in the same coordinates system, and its numerical solution procedure is assessed. We assume here that the magnitude and application range of the available friction is given by a step function. With the obtained solution, an algorithm is outlined for reaching a winding angle of 90° when passing the pole of the vessel according to a prescribed accuracy level. The result of this procedure is a curve that provides the required coefficient of friction as a function of the roving trajectory partition on which this friction is applied.

The impact of the modified roving trajectories on the structural performance of the pressure vessel is shortly assessed in section 4 where we propose a simplified method for estimating the strength reduction and the size of the area where this reduction applies on.

In section 5 we demonstrate the utilisation of non-geodesics on a pressure vessel design with a relatively low q factor. Both geometric and structural aspects are here evaluated.

2 Pressure Vessel Design

In this section we provide a short overview of the parameters and equations covering the design of isotensoid pressure vessels.

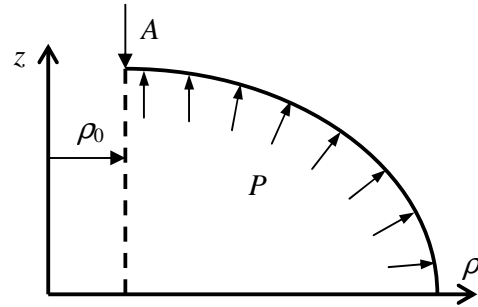


Fig. 1. Loads and geometry of pressure vessel meridian

2.1 Basic geometry

In figure 1, a schematic representation of an optimal meridian profile is given. When rotated around the z -axis, a shell of revolution can be obtained. The basic input parameters are the internal pressure P , the axial load A (as applied on the dome opening) and the radius of the polar opening, ρ_0 . In figure 2, the definition of the so-called winding angle is provided.

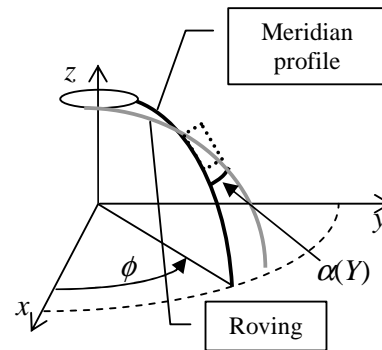


Fig. 2. Definition of winding angle and parallel angle

The shell is covered by geodesic trajectories, which are governed by the Clairaut equation [2]:

$$\sin \alpha(\rho) = \frac{\rho_0}{\rho} \quad (1)$$

Due to rotational symmetry, the shell will exclusively be loaded in-plane with an axial (z -direction) and tangential stress (peripheral direction). These loads depend on the ratio of the curvatures in these directions. The winding angle, as given by the Clairaut relation (1) should match the principal stress direction, as it is composed by the previously described membrane stresses. Matching the winding angle to the principal stress direction can only be achieved by the proper meridian geometry [2-5].

Without proceeding into details, the differential equation providing the optimal meridian shape is given by [4]:

$$Z'(Y) = \pm \frac{k_a Y + Y^3}{\sqrt{a^2 (Y^2 - 1) - (k_a Y + Y^3)^2}} \quad (2)$$

where:

$$\begin{aligned} Y &= \frac{\rho}{\rho_0}, & Z &= \frac{z}{\rho_0}, \\ a &= \frac{FN_f}{\pi P \rho_0^2}, & k_a &= \frac{A}{\pi P \rho_0^2} \end{aligned} \quad (3)$$

The symbol N_f stands for the total number of rovings crossing the equatorial periphery; each individual roving is loaded by a force F . The \pm sign in equation (2) indicates that the solution (integration) can generate both the upper and lower part of the meridian profile.

2.2 Solution interval

The meridian we look for can be obtained by integration of equation (2). The independent parameter Y must provide real positive values for the argument contained in the square root of the denominator. When solving this 6th degree equation, we obtain 2 double real, and a pair of imaginary roots [2]. The smallest and bigger real roots define the interval where integration of equation (2) is possible. Although the biggest real root (Y_{eq}) does provide feasible values for the radius at the equator, the smallest root (Y_{min}) does in general not coincide with the opening radius at the pole ($Y_{min} > 1$). On the other hand, to continue the winding process when

passing the polar area, the winding angle should be equal to exactly 90° , or, in other words, perfectly tangential to the polar opening periphery.

2.3 Parameterisation

As we will return later to the issue of the non-tangential roving placement at the pole, we will first introduce a new parameterisation for facilitating the integration of equation (2):

$$\begin{aligned} Y^2(\theta) &= Y_{eq}^2 \cos^2 \theta + Y_{min}^2 \sin^2 \theta \\ \text{where} \quad & -\frac{\pi}{2} \leq \theta \leq \frac{\pi}{2} \end{aligned} \quad (4)$$

In addition, we introduce:

$$q = \left(\frac{Y_{eq}}{Y_{min}} \right)^2, \quad r = \frac{k_a}{Y_{eq}^2} \quad (5)$$

By setting the denominator of equation (2) equal to zero and substituting (4) and (5), the minimum and maximum dimensionless radii can be expressed as follows:

$$\begin{aligned} Y_{min}(q, r) &= \frac{1}{\sqrt{q}} Y_{eq}(q, r) = \\ &= \frac{1}{\sqrt{q}} \sqrt{\frac{1 + q + 2qr + q^2(1+r)^2}{1 + q + 2qr}} \end{aligned} \quad (6)$$

For the dimensionless roving tension a , we obtain:

$$\begin{aligned} a(q, r) &= \frac{[1 + q + 2qr + q^2(1+r)^2]^{3/2}}{q(1 + q + 2qr)} \\ &= \frac{FN_f}{\pi P_r \rho_0^2} \end{aligned} \quad (7)$$

Returning to figure (1) and equation (2) it is evident that the meridian profile will only depend on two parameters: the dimensionless roving tension a and the dimensionless axial force k_a . The first parameter in fact expresses the strength of the applied roving as compared to the internal pressure, while the second one relates the true axial force to the total axial force generated by the internal pressure on the surface of the polar opening. The vector $\{a, k_a\}$ can, with the introduced

parameterisation, be replaced by $\{q, r\}$ which in essence expresses the same design parameters (roving loading and axial force magnitude). The $\{a, k_a\}$ vector is more convenient for initial design as it stays closer to the intuitive idea of loads and pressure, while the $\{q, r\}$ combination is more usable for direct calculation of the pressure vessel properties.

2.4 Meridian Shape

The original equation (2) has now to be transformed into the new independent parameter θ . Application of the chain rule leads to:

$$\begin{aligned} \frac{dZ}{d\theta} &= \frac{dZ}{dY} \frac{dY}{d\theta} = \\ &= Y_{\min} \frac{qr + q \cos^2 \theta + \sin^2 \theta}{\sqrt{1 + 2q(1+r) + (1-q)\sin^2 \theta}} \end{aligned} \quad (8)$$

After integration, we obtain:

$$\begin{aligned} Z(q, r, \theta) &= \frac{Y_{\min}}{\sqrt{1 + 2q(1+r)}} \times \\ &\times \left[(1 + 2q(1+r)) \operatorname{ellE} \left(\theta, \frac{q-1}{1 + 2q(1+r)} \right) - \right. \\ &\quad \left. (1 + q + qr) \operatorname{ellF} \left(\theta, \frac{q-1}{1 + 2q(1+r)} \right) \right] \end{aligned} \quad (9)$$

where $\operatorname{ellF}(\#_1, \#_2)$ and $\operatorname{ellE}(\#_1, \#_2)$ denote incomplete elliptic integrals of the first and second kind, respectively [3]. For a particular pressure–axial-load combination $\{q, r\}$ or $\{k_a, a\}$, the shape is parametrically described as a function of the independent coordinate θ . For the derivation of other important properties like the ϕ -coordinate development as a function of θ and the roving length, we will first introduce some concepts from differential geometry. These concepts are explained in the next section where we present the equation for non-geodesic winding on shells of revolution.

3 Non-geodesic trajectories

In this section we provide, without outlining the complete derivation, the differential equation governing non-geodesic trajectories on shells of revolution.

3.1 Coefficients of the First Fundamental Form

Let a surface be given by the following parameterisation:

$$\begin{aligned} \mathbf{S}(\theta, \phi) &= \{x(\theta, \phi), y(\theta, \phi), z(\theta, \phi)\} \\ \text{with } \theta, \phi &\in \mathfrak{R} \end{aligned} \quad (10)$$

The coefficients of the first fundamental form are [3]:

$$\begin{aligned} G &= \mathbf{S}_\theta \cdot \mathbf{S}_\theta \\ F &= \mathbf{S}_\theta \cdot \mathbf{S}_\phi \\ E &= \mathbf{S}_\phi \cdot \mathbf{S}_\phi \end{aligned} \quad (11)$$

where the subscript denotes “differentiation with respect to”. These coefficients express in essence the metrics as we run along the surface in the directions of the defining parameters θ and ϕ . In the case of a shell of revolution, the scalar G links the meridian metric to θ and E relates the periphery metric to ϕ (F is equal to zero due to the orthogonality of the main directions). In the case of the pressure vessel under consideration, the surface parameterisation is given by [3]:

$$\begin{aligned} \mathbf{S}(\theta, \phi) &= \\ &= \{Y(q, r, \theta) \cos \phi, Y(q, r, \theta) \sin \phi, Z(q, r, \theta)\} \quad (12) \\ \text{with } -\frac{\pi}{2} &\leq \theta \leq \frac{\pi}{2} \quad \text{and} \quad 0 \leq \phi \leq 2\pi \end{aligned}$$

With this definition, the E and G coefficients can directly be evaluated according to equation (11). For the differentiation of the Involved Y and Z functions we respectively refer here to equations (4) and (8).

3.2 Roving length and ϕ propagation

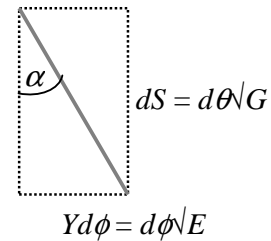


Fig. 3. The geometric relation between G , E and α .

In figure 2, at the point where the roving crosses the depicted meridian, an infinitesimally small square (dotted) is given. This square is expanded in figure 3 where we provide the definition of some characteristic metrics, as related to E , G and the winding angle α . From the figure it becomes clear that the roving length L co-dependes on α . The same applies on ϕ . The angle α can, in the case of geodesic winding be obtained by substitution of equation (4) into (1). The roving length differential is then given by [3]:

$$\begin{aligned} \frac{\partial L(q, r, \theta)}{\partial \theta} &= \frac{\sqrt{G(q, r, \theta)}}{\cos[\alpha(q, r, \theta)]} = \\ &= Y_{\min}^2(q, r) \sqrt{\frac{q(1+q+2qr)}{2+2q(1+r)+(q-1)\cos^2\theta}} \end{aligned} \quad (13)$$

Integration leads to:

$$\begin{aligned} L(q, r, \theta) &= Y_{\min}^2(q, r) \times \\ &\times \sqrt{\frac{q(1+q+2qr)}{1+2q(1+r)}} \operatorname{ellF}\left(\theta, \frac{q-1}{1+2q(1+r)}\right) \end{aligned} \quad (14)$$

This equation applies only on geodesic trajectories. The differential equation for ϕ is given by [3]:

$$\begin{aligned} \frac{\partial \phi(q, r, \theta)}{\partial \theta} &= \frac{\sqrt{G(q, r, \theta)}}{\sqrt{E(q, r, \theta)}} \tan[\alpha(q, r, \theta)] = \\ &= \frac{\sqrt{q}\sqrt{1+q+2qr}}{(q\cos^2\theta + \sin^2\theta)\sqrt{2+q+2qr(q-1)\cos^2\theta}} \end{aligned} \quad (15)$$

Integration leads to:

$$\begin{aligned} \phi(q, r, \theta) &= \sqrt{\frac{1+q+2qr}{q[1+2q(1+r)]}} \times \\ &\operatorname{ell}\Pi\left(\frac{q-1}{q}; \theta \middle| \frac{q-1}{[1+2q(1+r)]}\right) \end{aligned} \quad (16)$$

where $\operatorname{ell}\Pi(\#_1; \#_2 | \#_3)$ stands for an incomplete elliptic integral of the third kind. Once again, the provided solution is only valid for geodesics. We should stress here, that in the case of non-geodesic winding, the (yet) undefined angle α will additionally depend on the friction distribution (e.g. as a function of θ). The

corresponding expression for α is to be obtained by solving a non-linear differential equation.

3.3 Curvatures

In the case of non-geodesic roving trajectories, an essential ingredient for the calculation of the winding angle is the normal curvature of that trajectory. For a surface where the main curvature directions are orthogonal, the normal curvature can be composed by a combination of these main curvatures: the meridional (θ -direction) and parallel (ϕ -direction) curvature. These are given by:

$$\begin{aligned} k_m(q, r, \theta) &= \operatorname{sgn}(Y) \frac{Y_{\theta\theta}S_\theta - S_{\theta\theta}Y_\theta}{(Y_\theta^2 + S_\theta^2)^{3/2}} \\ k_p(q, r, \theta) &= \frac{-S_\theta}{|Y|(Y_\theta^2 + S_\theta^2)^{1/2}} \end{aligned} \quad (17)$$

where “sgn” stands for “sign”. With the two main curvatures known, the normal curvature is given by [3]:

$$k_n(q, r, \theta) = k_m \cos^2 \alpha + k_p \sin^2 \alpha \quad (18)$$

This expression is known as the Euler curvature equation. It is only valid for cases where the main curvature directions are perpendicular to each other. This condition does apply on shells of revolution.

3.4 Differential Equation for Non-Geodesics

Based on the definitions of the coefficients of the first fundamental form, we provide here (without derivation) the differential equation governing non-geodesic trajectories on shells of revolution [3]. Temporarily, it is assumed that the friction (μ) distribution is a function of the independent coordinate θ , hence $\mu(\theta)$:

$$\begin{aligned} \frac{d\alpha(\theta)}{d\theta} &= -\frac{1}{2} \frac{E_\theta(q, r, \theta)}{E(q, r, \theta)} \tan[\alpha(\theta)] + \\ &+ \mu(\theta) \frac{\sqrt{G(q, r, \theta)}}{\cos[\alpha(\theta)]} k_n(q, r, \theta) \end{aligned} \quad (19)$$

For zero friction, the solution is the well-known Clairaut equation (1). In every other case, the roving path will deviate from the geodesic one. It should be noted here that the sign before the friction function

in equation (19) could be negative as well. In this case the friction will tend to steer the roving path in the opposite direction.

3.5 Solution procedure

The main problem for pressure vessels with rather low q -values (the polar opening radius is not too small as compared to the equator radius) is the inability of the roving trajectory to reach a winding angle $\alpha = 90^\circ$ when passing the pole. This shortcoming makes continuation to a next wound circuit impossible. Therefore, by application of a partially non-geodesic roving path, this requirement must be met. An important condition for this modification is to ensure continuity of the winding angle as a function of θ at the point where it jumps to the non-geodesic part. This should be incorporated as the initial condition for solving equation (19).

A second condition is associated with the resulting winding angle propagation. Depending on the meridian profile geometry and the applied quantity of friction, the winding angle might become 90° before the roving has reached the polar area (more accurate, before the roving has reached the minimum vessel radius). When using a standard solver, e.g. Runge-Kutta (which is provided in standard mathematics packages), an additional routine must be incorporated for exactly achieving a 90° winding angle at the minimum radius (polar opening).

To demonstrate this procedure, we assume here that the friction is given by a step function:

$$\begin{aligned} \mu(\gamma, m, \theta) &= 0 & 0 \leq \theta \leq \gamma \\ \mu(\gamma, m, \theta) &= m & \gamma \leq \theta \leq \frac{\pi}{2} \end{aligned} \quad (20)$$

where m is the maximum friction available (usually around 0.1 to 0.3) and γ the θ -coordinate where the step takes place. We should note here that for the parameterisation used here (equation (4)) the equator is represented by $\theta = 0$. The step function assumed here is able to provide the complete range for friction influence, from zero to 100%. In addition, it has proven to provide sufficient stability for the solution of (19). Obviously, other functions can be used as well.

The goal is now to provide for every γ a corresponding friction value m that ensures a winding angle of 90° at exactly Y_{\min} ($\theta = \pi/2$). This

coefficient of friction must be determined up to a desired level of accuracy ε and must belong to a predetermined feasible friction interval $\{\mu_{\min}, \mu_{\max}\}$. For given γ and m , the solution procedure for equation (19) is initialised as follows (schematically):

$$\begin{aligned} (\text{input}) &= \begin{Bmatrix} q \\ r \\ \gamma \\ m \end{Bmatrix} \\ (\text{independent parameter}) &= \theta: 0 \leq \theta \leq \frac{\pi}{2} \\ (\text{initial condition}) &= \begin{Bmatrix} \alpha_{\text{ng}} = \arcsin\left(\frac{1}{Y_{\text{eq}}(q, r)}\right) \\ \text{at } \theta = 0 \end{Bmatrix} \\ \text{solution} &= \alpha_{\text{ng}}(q, r, \gamma, m, \theta) \end{aligned} \quad (21)$$

For a particular γ , the input value m (as implemented in equation (10)) might be too high or too low. In the first case, we will reach 90° before arriving at the pole, in the second case the roving will pass the pole with $\alpha < 90^\circ$. Depending on this result, the value m must accordingly be adjusted. The routine for performing this is very similar to iterative root searching methods (Newton). A pseudo code for this is provided here:

```

FUNCTION test( $\gamma$ )
 $a_0 = \mu_{\min}$ 
 $b_0 = \mu_{\max}$ 
WHILE  $|\alpha_{\text{ng}}(q, r, \gamma, m, (a_0+b_0)/2, \pi/2) - \pi/2| > \varepsilon$ 
DO
  IF  $|\alpha_{\text{ng}}(q, r, \gamma, m, (a_0+b_0)/2, \pi/2) - \pi/2| > 0$ 
  THEN
     $a_0 = a_0$ 
     $b_0 = (a_0+b_0)/2$ 
  ELSE
     $a_0 = (a_0+b_0)/2$ 
     $b_0 = b_0$ 
  ENDF
ENDWHILE
RETURN  $(a_0+b_0)/2$ 

```

(22)

The function *test* returns for every γ the proper coefficient of friction m within the prescribed accuracy ε . When ε is too small, the loop might not converge; therefore it is advisable to incorporate a second criterion in the *while* statement like an iteration counter with a prescribed limit.

4 Structural Performance Reduction

The design procedure for optimal meridian profiles is based on the assumption of utilising geodesic trajectories. After the performed correction to achieve the desired 90° winding angle at the pole, we have been forced to involve non-geodesic winding. As a result of this application, the roving orientation does not correspond to the optimal one anymore. Therefore the structural performance of the pressure vessel is reduced. To assess this reduction, a reconsideration of the differential equation for the optimal meridian profile is here necessary. Rewriting of equation (2) results in [2-5]:

$$a \left(\frac{\sqrt{Y^2 - 1}}{Y} \right) \left(\frac{Z'(Y)}{\sqrt{1 + Z'(Y)^2}} \right) = k_a + Y^2 \quad (23)$$

The first term between parentheses is associated with the winding angle. The second term within parentheses indirectly provides the slope of the meridian profile as a function of Y . Hence, another form for writing equation (23) is [3]:

$$a \cos \alpha \cos \beta = k_a + Y^2 \quad (24)$$

In this expression, the original winding angle α must be replaced by the non-geodesic one: $\alpha_{ng}(q, r, \gamma, m, \theta)$. As compared to the original setup (geodesic winding), the relative performance reduction δ can now be quantified as follows:

$$\delta(q, r, \gamma, m, \theta) = \frac{\cos[\alpha_{ng}(q, r, \gamma, m, \theta)]}{\cos[\alpha(q, r, \theta)]} \quad (25)$$

We should notice here that the meridian itself is not affected by non-geodesic winding, hence $\beta(\theta)$ remains the same. Nevertheless, we must state here that δ provides only a rough estimation for the performance reduction [5].

5 Results

In this section, the outlined theory is applied on a pressure vessel with $q = 3$ and $r = 0$ (no axial loading). Without any roving path modification, the winding angle at the poles is equal to about 72° , hence this item is not suitable for production.

5.1 Friction distribution

The first step is to utilise non-geodesic winding for achieving the desired winding angle at the polar opening (minimum radius). Taking the step function definition into consideration (equation (21)) the combinations (γ, m) must be determined on such a way that the roving will obtain an angle of 90° at exactly $Y_{\min} (\theta = \pi/2)$. The result (with $\varepsilon = 0.02^\circ$), after application of the routine (22), is given below (figure 4):

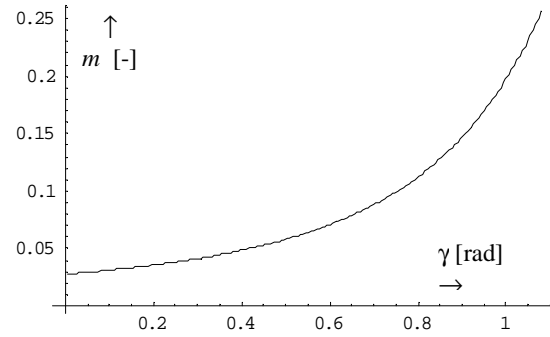


Fig. 4. Friction coefficient m for tangential fibre placement at the pole as a function of the step interval γ

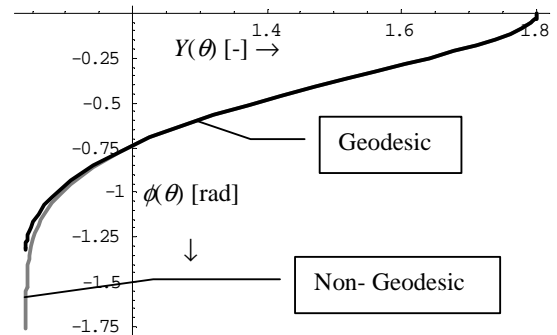


Fig. 5. Parallel angle propagation as generated by geodesic and non-geodesic winding

5.2 Geometric vessel properties

Based on figure 4, we arbitrary chose here for $\{\gamma = 1.0338, m = 0.219\}$. As the original winding angle is extended towards 90° , the roving path will cover a bigger range for the ϕ -angle (it shows the tendency to follow the periphery of the polar opening). From figure 5, it is clear that the total ϕ -propagation has increased from 1.27 to 1.76 [rad]. This increase has a great influence on the eventual derivation of a suitable winding pattern.

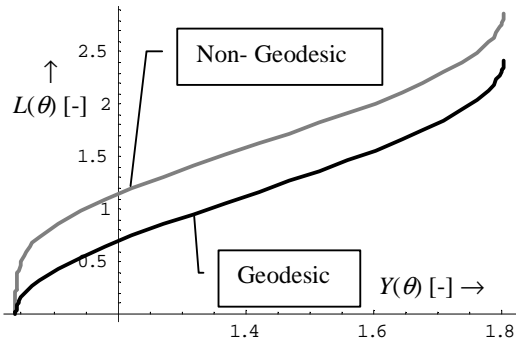


Fig. 6. Roving length as generated by geodesic and non-geodesic winding

The increased ϕ -propagation of the roving trajectory implies also an increased overwound roving length. This can be viewed in figure 6. From the figure it is clear that the increase in roving length is mainly located around the polar area, figure 7:

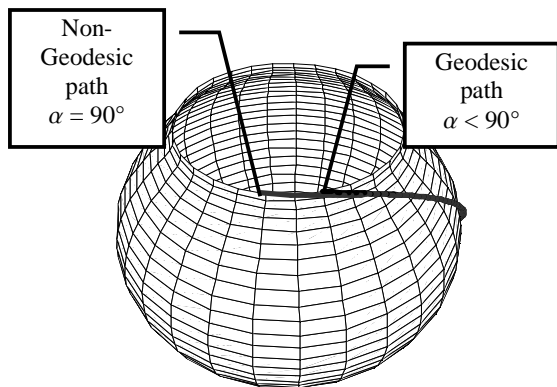


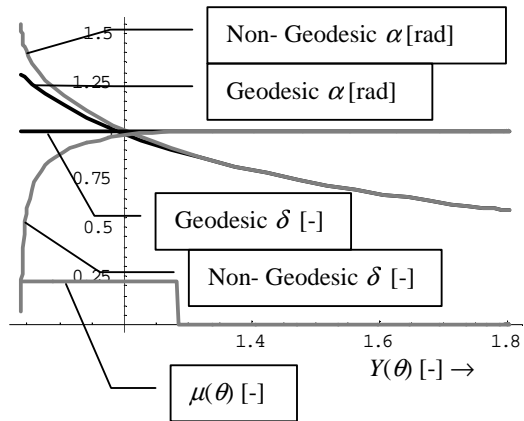
Fig.7. Geodesic (black) and adapted non geodesic path (grey) for reaching a winding angle of 90° , both applied on an optimal meridian profile for pressure vessels

The graphs for $\phi(\theta)$ and $L(\theta)$ have been evaluated by performing numerical integration on the first line (that contains E and G) of equations (13) and (15) respectively, after substitution of $\alpha_{ng}(q, r, \gamma, m, \theta)$.

5.3. Structural performance

As previously mentioned, due to the modified roving orientation, the structural performance of the vessel is expected to be less than the optimal one. In figure 8, we observe that at the point where the friction step function becomes active, the structural performance starts reducing. At exactly the pole, the performance drops to zero. Fortunately, in practice, this area is usually reinforced by a flange. In addition, the thickness build up, as observed on typical pressure vessel configurations, is able to partially alleviate the lack of roving-force-internal-pressure equilibrium. Nevertheless, when designing a flange, the strength reduction along the Y -axis must certainly be taken into consideration.

Fig.8. Winding angles and performance reduction due to non-geodesic winding



6 Conclusions

In this paper we have presented a methodology for the calculation of non-geodesic roving trajectories on typical isotensoid pressure vessels with a specific application in mind: tailoring the winding angle at the pole to become exactly equal to 90° for ensuring winding-ability. In other words, by creating a perfect tangential roving passage at the pole, continuation to the following wound circuits does become in this case feasible. Since this non-tangentiality condition is almost typical for every pressure vessel design, the authors believe this paper tackles a realistic problem while providing directly

usable solutions. Moreover, the presented methodology is directly coupled to the analytical design parameterisation procedure of such vessels and has a straightforward character.

After a short presentation of the composite pressure vessel design theory (netting), some basic geometry parameters have been explained. With these parameters, the differential equation for non-geodesic trajectories has been outlined. With the proper initialisation and a dedicated algorithm for determining the friction distribution characteristics that fulfil the tangentiality condition, a simplified method has been derived for the estimation of the strength reduction (as a result of the modified roving trajectories). The method has been demonstrated on a typical pressure vessel design case where both geometric and structural characteristics have been evaluated.

The proposed methodology for non geodesic trajectories, specifically applied on isotenoid composite pressure vessels, performs very well in terms of accuracy, flexibility and computational demands. It provides a straight forward tool for immediate assessment of possible design configurations. At the same time, the generated coordinates can immediately be used for the elaboration of winding patterns and the determination of CNC data for controlling winding machines.

References

- [1] Beukers A, Hinte E van. *Lightness: The inevitable renaissance of minimum energy structures*. Rotterdam: 010 Publishers, 1998.
- [2] Jong de Th. *A theory of filament wound pressure vessels*. Report LR-379. Structures and materials laboratory, Faculty of Aerospace Engineering, Delft University of Technology. Delft, April, 1983.
- [3] Koussios S. *Filament Winding: a Unified Approach*. PhD Thesis Report. Desing & Production of Composite Structures, Faculty of Aerospace Engineering, Delft University of Technology. Delft University Press, 2004.
- [4] Nieuwenhuizen E. *Composite LPG fuel containers for motor vehicles*. M.Sc. thesis report. Structures and materials laboratory, Faculty of Aerospace Engineering, Delft University of Technology. Delft, August, 1995.
- [5] Koussios S, Bergsma OK. Isotenoid Pressure Vessels Based on Non-Geodesic Trajectories. *15th International Conference on Composite Materials*. Durban, South Africa, June-July, 2005.
- [6] Gray A. *Modern Differential Geometry of Curves and Surfaces*. CRC press, 1993.
- [7] Koussios S, Bergsma OK, Beukers A. Filament Winding Part 1: Determination of the Wound Body Related Parameters. *Composites Part A: Applied Science and Manufacturing* 2004; 35: 181-195.
- [8] Koussios S, Bergsma OK, Beukers A. Filament Winding Part 2: Generic Kinematic Model and its Solutions. *Composites Part A: Applied Science and Manufacturing* 2004; 35: 197-212.